Pressure−Temperature Phase Transition Diagram for Wheat Starch

J. P. Douzals,[†] J. M. Perrier-Cornet,[†] J. C. Coquille,[‡] and P. Gervais*,[†]

ENSBANA, 1 Esplanade Erasme, F-21000 Dijon, France, and ENESAD, Boulevard O. de Serres,
21800 Quétigny, France

Wheat starch suspensions in water (5% dry matter) were subjected to various pressures (0.1−600 MPa) and temperatures (−20 to 96 °C) for 15 min. The gelatinization rate was measured after treatment by using microscopic measurements of the loss of birefringence of the granules. This method was previously calibrated by differential scanning calorimetry. Curves of isogelatinization were found to be quite similar to a pressure−temperature (*P*−*T*) diagram of unfolding proteins. Results were first analyzed by considering the thermodynamic aspects related to the d*T*/d*P* curve shifts. On the basis of equations already shown for proteins, the *P*−*T* gelatinization diagram of wheat starch would show different kinds of thermal contributions, suggesting endothermic, athermic, or exothermic melting reactions. Second, as a practical consequence, these previous *P*−*T* areas corresponded to specific gelatinization conditions as confirmed by hydration evaluation measured by starch swelling index. Depending on the pressure−temperature conditions, gelatinization would involve hydration. Lowering the pressure and temperature resulted in a complete gelatinization with less hydration in comparison with a thermal treatment at atmospheric pressure. A hydration model based on an energetic approach was proposed.

Keywords: *Starch gelatinization; high hydrostatic pressure; phase diagram; hydration*

INTRODUCTION

Starch gelatinization corresponds to a combined mechanism of semicrystalline polymer melting (*1*) and hydration (*2*) because gelatinization occurs only in an aqueous medium. From thermodynamics, the effects of pressure and/or temperature on the melting equilibrium of a pure solid are described by the Clausius−Clapeyron equation

$$(\mathrm{d}T/\mathrm{d}P)_{\Delta G=0} = \Delta S/\Delta V \qquad (1)$$

where ΔG is the Gibbs free energy (J mol^{-1}), d*T* is the temperature variation (K), d*P* is the pressure variation (Pa), ΔV is the volume shift during the process (m^3), and ΔS is the transition entropy (J mol^{-1} K^{-1}).

Melting is generally an endothermic reaction for a pure solid, which is followed by an increase in volume between liquid and solid phases. Consequently, the d*T*/d*P* slope given by eq 1 is generally positive and an increase in pressure is not favorable for melting at low temperatures. Examples of positive d*T*/d*P* slope have been shown for macromolecules such as κ-carraghenan (*3*), some lipids (*4*), and starch (*5*).

The opposite result (negative d*T*/d*P* slope) has been found for agarose because the gel−sol transition induces a reduction of the total volume (*6*).

Water is a natural solvent for macromolecules, and the solid−liquid transition exhibits a specific behavior with a negative d*T*/d*P* curve below 210 MPa (negative ΔV) and a positive d*T*/d*P* slope above 210 MPa (positive

ΔV) (*7*). However, these two transitions do not involve the same products (respectively Ice-types Ih and III).

Pressure−temperature (*P*−*T*) phase transition diagrams of some proteins were extensively studied by unfolding and denaturing under pressure (*8*−*10*). These authors showed that there is a nonmonotonic evolution of the transition curve as shown by

$$\Delta G - \Delta G_0 = -RT \ln \frac{K}{K_0} = \Delta V_0(P - P_0) - \Delta S_0(T - T_0) + 2\Delta\alpha(P - P_0)(T - T_0) + \frac{\Delta K}{2}(P - P_0) - \frac{\Delta C_p}{2T_0}(T - T_0) \quad (2)$$

where ΔG is the Gibbs free energy (J mol^{-1}), K is the reaction rate (mol^{-1}), ΔV_0 is the volume variation (m^3), ΔS_0 is the entropy variation (J mol^{-1} K^{-1}), $\Delta\alpha$ is the thermal expansion variation (m^3 K^{-1}), $\Delta\beta$ is the compressibility variation (m^3 MPa^{-1}), and ΔC_p is the heat capacity variation (J g^{-1} K^{-1}).

The transition curve described by eq 2 corresponds to an elliptical curve in the *T*−*P* plane. The shifts ΔS, ΔV, $\Delta\beta$, $\Delta\alpha$, and ΔC_p correspond to variations between reactants and products (i.e., before and after the transition) as shown in Figure 1. ΔS and ΔV correspond to the energetic changes of the products due to temperature or pressure variations. As shown in Figure 1, ΔS and ΔV might be positive or negative depending on the *P* and *T* values. $\Delta\alpha$, $\Delta\beta$, and ΔC_p correspond to modifications between the native and denatured states.

To study the effects of high pressure on starch gelatinization, numerous authors have used the Clausius−Clapeyron equation, by considering starch gelatinization as a phase transition (*5, 11, 12*).

The first studies were carried out using high-pressure

---

* Author whom correspondence should be addressed [telephone +33 (0)380 396 654; fax +33 (0)380 396 611; e-mail gervais@u-bourgogne.fr].
† ENSBANA.
‡ ENESAD.

874 *J. Agric. Food Chem.,* Vol. 49, No. 2, 2001

Douzals et al.
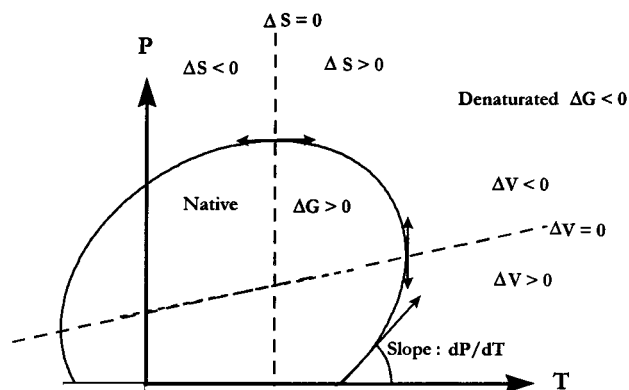
Figure 1. Theoretical pressure−temperature diagram of protein denaturing (*8*).

differential thermal analysis (HPDTA) (*11*). These authors studied the evolution of the dT/dP slope (described by eq 1) for various pressures and showed how ΔV evolves between reactants and products. Below 200 MPa, ΔV appeared to be positive but became negative above 300 MPa for wheat and potato starches. These results correspond to an inflection in the dT/dP slope (eq 1).

Similar results have been obtained for wheat starch by Thevelein et al. (*5*), who found an increase in the melting temperature with increasing pressure below 200 MPa. Other work has shown that gelatinization of wheat starch granules occurs for pressures >300 MPa, at 25 °C. The total gelatinization of wheat starch was found to occur at 600 MPa, 25 °C, applied for 15 min (*13*). Pressure-induced products obtained at room temperature showed specific properties related to the contraction of the suspension volume (i.e., specific gravity or Young modulus), in comparison with a thermal treatment at 86 °C, 15 min (*14*). This last study showed that the intensity of heat or pressure gelatinization was closely related to hydration. However, a high-pressure treatment induced less hydration [as measured by swelling index (*15*)] than a thermal treatment for an equivalent degree of gelatinization, as determined by differential scanning calorimetry (DSC).

Previous studies mainly focused on a comparison between pressure and temperature effects on starch gelatinization. First, one aim of this paper is to show eventual cooperative or antagonistic effects of P–T combined treatments. Starch gelatinization after treatment was evaluated by using DSC and the loss of birefringence of starch granules. The results from these measurements were used to obtain a P–T gelatinization diagram of wheat starch. Second, we identified specific areas in the P–T diagram where thermodynamics suggest particular conditions for starch gelatinization. Finally, starch hydration was evaluated after treatment for different regions of the P–T diagram. These measurements confirmed previous results. That is, the specific P–T areas suggested by thermodynamics were characterized by a greater or lesser degree of hydration.

MATERIALS AND METHODS

Starch Suspensions and Treatment Conditions. Commercial wheat starch was used in this study and provided by Prolabo, France. Wheat starch powder was 88% dry matter (DM), as verified in a dry air oven at 105 °C during 48 h, and 23% amylose content, as checked by iodine titration.

Starch suspensions were prepared with 5% DM (on a dry matter basis) with distilled water and sealed in rubber bags of ~15 mL volume (60 mm length and 18 mm diameter).

Thermal treatments were applied from −20 to 96 °C in a water bath. Pressure treatments varied from 0.1 to 600 MPa using an isostatic high-pressure equipment described elsewhere (*13*). When pressure was combined with low or high temperatures, a 5 mL high-pressure cell was placed in a controlled-temperature bath in the range of −25 to 100 °C. Each treatment was applied for 15 min when the desired pressure and temperature were reached. In the case of combined treatments, final pressures and temperatures were reached by steps of ±100 MPa and ±5 °C in reference to initial conditions (0.1 MPa and 20 °C).

Calorimetric Evaluation of Starch Gelatinization. Starch gelatinization was checked using DSC after treatment. About 10 mg of starch suspensions (5% DM) was sealed into DSC pans (6 mm diameter and 3 mm thin) and heated at 10 °C min^{-1} from 20 to 130 °C. The DSC apparatus was a Perkin-Elmer DSC II calibrated with indium. Melting enthalpies were manually determined with a precision of ±0.5 J g^{-1} of DM. Each sample was heated twice, but relevant results were obtained only during the first heating. Each experiment was independently repeated three times.

Optical Analysis of Granule Gelatinization. Starch gelatinization was also checked after treatment by the loss of optical birefringence of starch granules. Wheat granule birefringence was checked using an inverted light microscope provided with a polarization analyzer. The melted fraction was determined by the number of granules that lost their birefringence divided by the total number of starch granules.

One hundred starch granules were counted three times. Precision in melted fraction determination was ~5%.

Hydration Measurements. Starch hydration was measured after a thermal and/or pressure treatment using the swelling index method described by Doublier (*15*) and Douzals et al. (*14*). All experiments were realized in a large excess of water (5% DM). The swelling index was determined by the amount of water bound to insoluble dry matter. Starch products were centrifuged at 2000 rpm for 5 min at 25 °C. Supernatants were isolated, and DM was measured upon dried pellets. The swelling index is given in grams of water per gram of DM with a precision of ±1 g of H_2O/g of DM.

RESULTS AND DISCUSSION

Gelatinization Intensity Calibration. Because a P–T gelatinization diagram encompasses a large number of experimental data, gelatinization was evaluated optically from the loss of birefringence of the starch granules after treatment. Microscopic determination of starch gelatinization was initially calibrated with DSC for a range of pressures (0.1−600 MPa, 25 °C, 15 min) or temperatures (25−76 °C, 15 min, 0.1 MPa). The results presented in Figure 2 show a constant lag between the two methods because the optical method always overestimates (~20%) the melted fraction in comparison with DSC results after the same pressure or temperature treatment. Previous high-pressure or thermal treatment did not significantly modify the lag shown in Figure 2.

These results were consistent with previous works (*16*) in which DSC thermograms were compared with optical measurements. Because DSC is a macroscopic measurement method, it became partially unusable when only a few granules were melted. Moreover, wheat starch has a relatively low melting enthalpy (17 J g^{-1} DM at 30% DM). On the other hand, optical measurements indicated physical modifications of the semicrystalline structure of starch granules. Such a microscopic method was able to show gelatinization of a small number of starch granules. Then, from a practical point

P–T Phase Transition for Starch

J. Agric. Food Chem., Vol. 49, No. 2, 2001 **875**
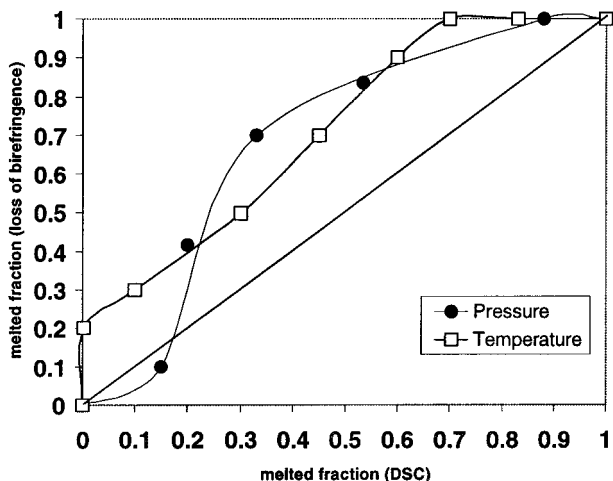
Figure 2. Comparison between DSC and granule loss of birefringence to evaluate starch gelatinization after thermal treatment at 0.1 MPa or pressure treatment at 25 °C during 15 min.
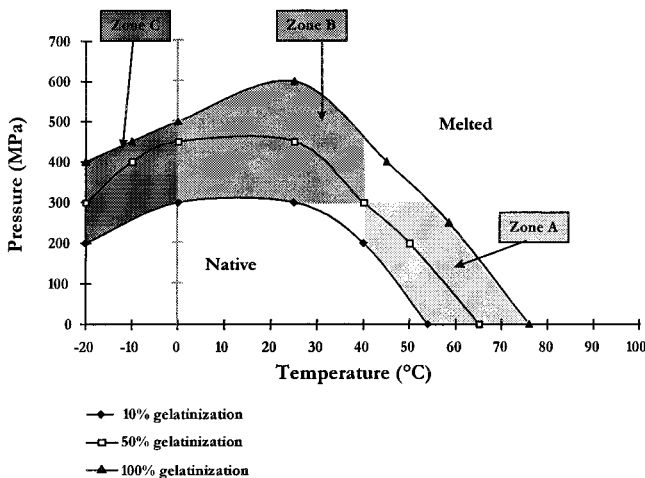
Figure 3. Pressure–temperature gelatinization diagram of wheat starch. Starch suspensions were 5% DM and treated during 15 min.

of view, DSC was used to characterize starch gelatinization along the pressure axis (at 25 °C) and temperature axis (at 0.1 MPa) of the diagram, whereas optical measurements were mostly employed for measurements outside the two axes.

Case of Combined Pressure–Temperature Treatments. Results obtained for 52 points were plotted on a *P–T* diagram, shown in Figure 3. As mentioned earlier, the gelatinization (melting) rate was determined using either DSC or loss of birefringence of the granules, and isogelatinization curves were drawn for 10, 50, and 100% of gelatinization. As shown in Figure 3, gelatinization rates were dependent on pressure and temperature conditions corresponding to a second-order model, similar to that described by eq 2. In accordance with eq 2, pressure mostly influences volume and compressibility variations between native and denaturated states, in agreement with Le Chatelier's principle. On the other hand, temperature influences entropy and heat capacity variations between native and denaturated states. Therefore, pressure and temperature variations involve volume as well as entropy variations in the gelatinization process as described by the d*T*/d*P* curve of the diagram shown in Figure 3.

The first area (zone A, Figure 3) corresponds to high temperatures from about 40 to 76 °C and low pressures (<300 MPa). Inside this area, an increase in pressure of 100 MPa resulted in a decrease in melting temperature of −7 °C for the same degree of gelatinization. The result is a negative d*T*/d*P* slope that indicates the favorable effect of pressure in lowering gelatinization temperature. As confirmed by DSC, starch gelatinization inside zone A was endothermic (positive Δ*S*). The relevant effect of the increasing pressure would indicate that starch gelatinization is realized with a negative Δ*V*. Indeed, the products (denatured state) would occupy a lower volume than the reactants (native state), that is, water and starch in suspension in the same conditions (*13*).

The second area (zone B, Figure 3) corresponded to the horizontal part of the curves located at higher pressures (>300 MPa) and between 0 and 40 °C.

These curves indicate that there is almost no influence of temperature on the gelatinization process. Previous studies indicated no melting entropy after a 500−600 MPa treatment for wheat starch (*13*). According to eq 2 and under these conditions of pressure and temperature, the starch gelatinization is athermic (Δ*S* = 0) and involves a negative Δ*V* of reaction. Such a behavior was also suggested for protein denaturation in aqueous medium (*8, 10*).

The third area (zone C, Figure 3) corresponded to subzero temperatures from 0 to −20 °C, where an increase in pressure of 100 MPa resulted in an increase in melting temperature of ∼+20 °C. In this last case, Δ*S* would be positive, suggesting that an exothermic reaction has occurred. This could be verified only by using DSC under high pressure.

Nevertheless, all of the experiments described in this paper concerned *P–T* treatments applied for 15 min: gelatinization kinetics were intentionally not studied. The results presented in this paper corresponded to a post-treatment evaluation of the gelatinization.

Gelatinization conditions described by zone A, B, or C involve specific functional properties. Previous works (*14*) showed significant differences in terms of functional properties for a single pressure (zone B) or single thermal treatments (zone A). As a first contribution, swelling indices were measured after the 52 previous treatments.

Hydration Levels for Combined *P–T* Treatments. The evolution of hydration versus pressure and temperature is introduced in Figure 4, which also includes the 100% melting curve. It is interesting to note that a complete gelatinization was obtained with ∼12 g of water/g of insoluble matter at 76 °C, 0.1 MPa.

The same gelatinization rate was obtained with 6 g of water/g of insoluble matter after 600 MPa, 25 °C, and <4 g of water/g of insoluble matter was measured after −15 °C, 400 MPa.

It is apparent from Figure 4 that higher pressures and lower temperatures always lower starch hydration at the same gelatinization rate. Although gelatinized granules consist of a heterogeneously hydrated system, we have considered a uniform hydration of starch by using the logical relationship between hydration and the evolution of internal energy. An energetic model was developed as described by the eq 3

$$U_{P,T} = U_{P_0, T_0} - \int p\Delta V + \int T\Delta S + \sum (ni_w U_w)_{P,T} \quad (3)$$
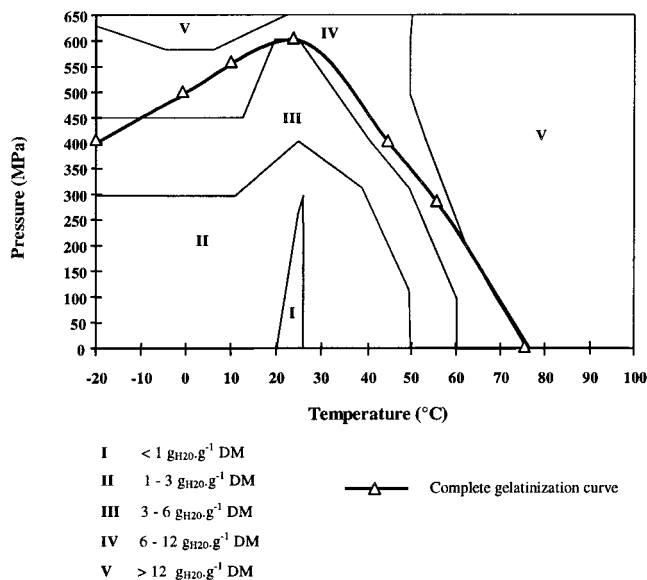
Figure 4. Hydration of wheat starch after pressure and temperature treatments. Hydration was measured on insoluble dry matter (swelling index), and initial suspensions were 5% DM.

where $U_{P,T}$ is the internal energy of the starch granule system, U_{P_0,T_0} is the internal energy at normal conditions, $\sum(ni_w U_w)$ is the energy fraction due to the number of hydration moles, and $-p\Delta V$ and $T\Delta S$ are the energy variations respectively due to pressure and temperature variations.

A comparison of eq 3 and Figure 3 shows that an increase in temperature always leads to an increase in internal energy $U_{P,T}$ (zone A, Figure 3). On the other hand, an increase in pressure always leads to a decrease in $U_{P,T}$ (zone B, Figure 3). When high pressure and cooling are combined, both parameters lead to a decrease in $U_{P,T}$ accordingly to eq 3. Then, in these last conditions, the hydration level would be lower (zone C, Figure 3).

Conclusion. This paper shows the effects of combined pressure–temperature treatments on starch gelatinization that occurs under different conditions of temperature and pressure.

Similarities between starch gelatinization and protein unfolding diagrams suggest peculiar effects of pressure on gelatinization at high or low (even negative) temperatures. Modifications of the dT/dP slope suggest that pressure–temperature conditions converted the original endothermic reaction into an a- or exothermic reaction. Nevertheless, these hypotheses must be checked using a high-pressure calorimeter.

Different areas of the $P-T$ gelatinization diagram were identified, and these represented specific properties depending on the gelatinization conditions. This was confirmed by an evaluation of starch hydration after treatment, which showed that complete gelatinization occurred with hydration levels which varied from 1 to 3. Starch hydration seems to follow an energy law based on the internal energy dependence on pressure and temperature.

Definition of a $P-T$ gelatinization diagram for wheat starch may find practical applications in process optimization and new product development. Each $P-T$ area (zone) might involve specific functional properties that would be interesting to explore.

LITERATURE CITED

(1) Lelievre, J. Theory of gelatinization in starch-water-solute system. *Polymer* **1976**, *17*, 854−858.

(2) Eliasson, A. C. Effects of water content on starch gelatinization. *Starch* **1980**, *32*, 270−272.

(3) Gekko, K. The sol−gel transition of macromolecules under pressure. In *Food Hydrocolloids: Structures, Properties and Functions*; Nishinari, K., Doi, E., Eds.; Plenum Press: New York, 1994; pp 259−264.

(4) Winter, R.; Czeslik, C. Lateral organization and phase behavior of phospholipid mixtures at high pressure. In *High Pressure Research in the Biosciences and Biotechnology*; Heremans, K., Ed.; Leuven University Press: Louvain, Belgium, 1997; pp 163−166.

(5) Thevelein, J. M.; Van Assche, J. A.; Heremans, K.; Gerlsma, S. Y. Gelatinization temperature of starch, as influenced by high pressure. *Carbohydr. Res.* **1981**, *93*, 304−307.

(6) Gekko, K.; Fukamizu, M. Effect of pressure on the sol−gel transition of gelatin. *Agric. Biol. Chem.* **1991**, *55*, 2427−2428.

(7) Franks, F. The properties of ice. In *Water, a Comprehensive Treatise*; Franks, F., Eds.; Plenum Press: New York, 1972; Vol. 1, pp 115−149.

(8) Hawley, S. A. Reversible pressure−temperature denaturation of chymotrypsogen. *Biochemistry* **1971**, *10*, 2436−2442.

(9) Heremans, K. High pressure effects on proteins and other biomolecules. *Annu. Rev. Biophys. Bioeng.* **1982**, *11*, 1−21.

(10) Kunugi, S. Modification of polymer functions by high pressure. *Prog. Polym. Sci.* **1993**, *18*, 805−813.

(11) Muhr, A. H.; Blanshard, J. M. V. Effects of hydrostatic pressure on starch gelatinisation. *Carbohydr. Polym.* **1982**, *2*, 61−74.

(12) Muhr, A. H.; Wetton, R. E.; Blanshard, J. M. V. Effect of hydrostatic pressure on starch gelatinisation, as determined by DTA. *Carbohydr. Polym.* **1982**, *2*, 91−102.

(13) Douzals, J. P.; Marechal, P. A.; Coquille, J. C.; Gervais, P. Microscopic study of starch gelatinization under high hydrostatic pressure. *J. Agric. Food Chem.* **1996**, *44*, 1403−1408.

(14) Douzals, J. P.; Perrier-Cornet, J. M.; Gervais, P.; Coquille, J. C. High-pressure gelatinization of wheat starch and properties of pressure-induced gels. *J. Agric. Food Chem.* **1998**, *46*, 4824−4829.

(15) Doublier, J. L. Rheological studies on starch flow behavior of wheat starch pastes. *Starch* **1981**, *33*, 425−420.

(16) Zanoni, B.; Schiraldi, A.; Simonetta, R. A native model of starch gelatinization kinetics. *J. Food Eng.* **1995**, *24*, 25−33.